AFRL-RX-WP-JA-2015-0093

CRITICAL PERCOLATION STRESSES OF RANDOM FRANK-READ SOURCES IN MICROMETER-SIZED CRYSTALS OF SUPERALLOYS (POSTPRINT)

M. D. Uchic, P. A. Shade, C. Woodward, and D. M. Dimiduk
AFRL/RXCM

S. I. Rao and T. A. Parthasarathy
UES, Inc.

APRIL 2014
Interim Report

AIR FORCE RESEARCH LABORATORY
MATERIALS AND MANUFACTURING DIRECTORATE
WRIGHT-PATTERSON AIR FORCE BASE OH 45433-7750
AIR FORCE MATERIEL COMMAND
UNITED STATES AIR FORCE

NOTICE AND SIGNATURE PAGE

Using Government drawings, specifications, or other data included in this document for any purpose other than Government procurement does not in any way obligate the U.S. Government. The fact that the Government formulated or supplied the drawings, specifications, or other data does not license the holder or any other person or corporation; or convey any rights or permission to manufacture, use, or sell any patented invention that may relate to them.

Qualified requestors may obtain copies of this report from the Defense Technical Information Center (DTIC) (http://www.dtic.mil).

AFRL-RX-WP-JA-2015-0093 HAS BEEN REVIEWED AND IS APPROVED FOR PUBLICATION IN ACCORDANCE WITH ASSIGNED DISTRIBUTION STATEMENT.

//Signature//

MICHEAL E. BURBA, Project Engineer
Metals Branch
Structural Materials Division

//Signature//

DANIEL J. EVANS, Chief
Metals Branch
Structural Materials Division

//Signature//

ROBERT T. MARSHALL, Deputy Chief
Structural Materials Division
Materials And Manufacturing Directorate

This report is published in the interest of scientific and technical information exchange and its publication does not constitute the Government's approval or disapproval of its ideas or findings.

REPORT DOCUMENTATION PAGE

Form Approved
OMB No. 0704-0188

1. REPORT DATE *(DD-MM-YY)*	2. REPORT TYPE	3. DATES COVERED *(From - To)*
April 2014	Interim	19 March 2014 – 31 March 2014

4. TITLE AND SUBTITLE
CRITICAL PERCOLATION STRESSES OF RANDOM FRANK–READ SOURCES IN MICROMETER-SIZED CRYSTALS OF SUPERALLOYS (POSTPRINT)

5a. CONTRACT NUMBER
In-house

5b. GRANT NUMBER

5c. PROGRAM ELEMENT NUMBER
62102F

6. AUTHOR(S)
M. D. Uchic, P. A. Shade, C. Woodward, and D. M. Dimiduk - AFRL/RXCM
S. I. Rao and T .A. Parthasarathy - UES, Inc.

5d. PROJECT NUMBER
4349

5e. TASK NUMBER

5f. WORK UNIT NUMBER
X0W6

7. PERFORMING ORGANIZATION NAME(S) AND ADDRESS(ES)

AFRL/RXCM
2941 Hobson Way
Bldg 654, Rm 136
Wright-Patterson AFB, OH 45433

UES Inc.
4401 Dayton-Xenia Rd.
Dayton, OH 45432-1894

8. PERFORMING ORGANIZATION REPORT NUMBER

9. SPONSORING/MONITORING AGENCY NAME(S) AND ADDRESS(ES)
Air Force Research Laboratory
Materials and Manufacturing Directorate
Wright-Patterson Air Force Base, OH 45433-7750
Air Force Materiel Command
United States Air Force

10. SPONSORING/MONITORING AGENCY ACRONYM(S)
AFRL/RXCM

11. SPONSORING/MONITORING AGENCY REPORT NUMBER(S)
AFRL-RX-WP-JA-2015-0093

12. DISTRIBUTION/AVAILABILITY STATEMENT
Distribution Statement A. Approved for public release; distribution unlimited.

13. SUPPLEMENTARY NOTES
Journal article published in *Modelling Simul. Mater. Sci. Eng.* 20 (2012) 065001 (7pp). ©2012 IOP Publishing Ltd. The U.S. Government is joint author of the work and has the right to use, modify, reproduce, release, perform, display or disclose the work. This report contains color. The final publication is available at doi:10.1088/0965-0393/20/6/065001.

14. ABSTRACT
2D dislocation dynamics simulations were used to investigate the size effect observed experimentally in the yield behavior of micrometer-sized crystals of γ–γ' superalloys. Random Frank–Read sources were introduced on a (1 1 1) glide plane for three simulation cell sizes. Critical stresses were determined for the percolation of dislocations evolving from the Frank–Read sources in such cells populated with a distribution of γ' precipitates at ~73.5% by volume, consistent with the experiment. An APB energy of 250 mJ m^{-2} was used in the simulations. The study found that the simulation results of percolation stresses were consistent with experimental 0.2% yield stress values with respect to both the scatter at each sample size, as well as the weak variation in critical stress with size. The weak size effect and the large scatter were found to be related to two factors: (1) strength of single-arm sources, as well as (2) the variation in precipitate structure at the single-arm source positions.

15. SUBJECT TERMS
dislocation dynamics, nickel-based superalloys, ParaDiS

16. SECURITY CLASSIFICATION OF:			17. LIMITATION OF ABSTRACT:	18. NUMBER OF PAGES	19a. NAME OF RESPONSIBLE PERSON (Monitor)
a. REPORT	b. ABSTRACT	c. THIS PAGE			Micheal E. Burba
Unclassified	Unclassified	Unclassified	SAR	10	19b. TELEPHONE NUMBER *(Include Area Code)* (937) 255-9795

Modelling Simul. Mater. Sci. Eng. **20** (2012) 065001 (7pp) doi:10.1088/0965-0393/20/6/065001

Critical percolation stresses of random Frank–Read sources in micrometer-sized crystals of superalloys

S I Rao[1], M D Uchic[2], P A Shade[2], C Woodward[2], T A Parthasarathy[1] and D M Dimiduk[2]

[1] UES, Inc., 4401 Dayton-Xenia Rd, Dayton, OH 45432-1894, USA
[2] Air Force Research Laboratory, Materials and Manufacturing Directorate, AFRL/MLLM Wright-Patterson AFB, OH 45433-7817, USA

Received 22 February 2012
Published 9 July 2012
Online at stacks.iop.org/MSMSE/20/065001

Abstract

2D dislocation dynamics simulations were used to investigate the size effect observed experimentally in the yield behavior of micrometer-sized crystals of γ–γ' superalloys. Random Frank–Read sources were introduced on a (1 1 1) glide plane for three simulation cell sizes. Critical stresses were determined for the percolation of dislocations evolving from the Frank–Read sources in such cells populated with a distribution of γ' precipitates at ~73.5% by volume, consistent with the experiment. An APB energy of 250 mJ m^{-2} was used in the simulations. The study found that the simulation results of percolation stresses were consistent with experimental 0.2% yield stress values with respect to both the scatter at each sample size, as well as the weak variation in critical stress with size. The weak size effect and the large scatter were found to be related to two factors: (1) strength of single-arm sources, as well as (2) the variation in precipitate structure at the single-arm source positions.

(Some figures may appear in colour only in the online journal)

1. Introduction

Experimental studies have shown that micrometer-scale face-centered cubic (fcc) crystals display strong strengthening effects, even at high initial dislocation densities [1–3]. Similar behavior has been observed for microcrystals of two-phase superalloys [4]. Previously, large-scale 3D discrete dislocation simulations (DDS) were used to explicitly model the pure compression deformation behavior of fcc materials under single-slip conditions [5–8]. A simulation study showed that two size-sensitive athermal hardening processes, beyond forest hardening, are *sufficient* to develop the dimensional scaling of the flow stress, stochastic stress variation, flow intermittency and high initial strain-hardening rates, similar to experimental observations for various fcc materials [5, 9]. One mechanism, source-truncation hardening, is especially potent in micrometer-scale volumes [5]. A second mechanism, termed exhaustion

0965-0393/12/065001+07$33.00

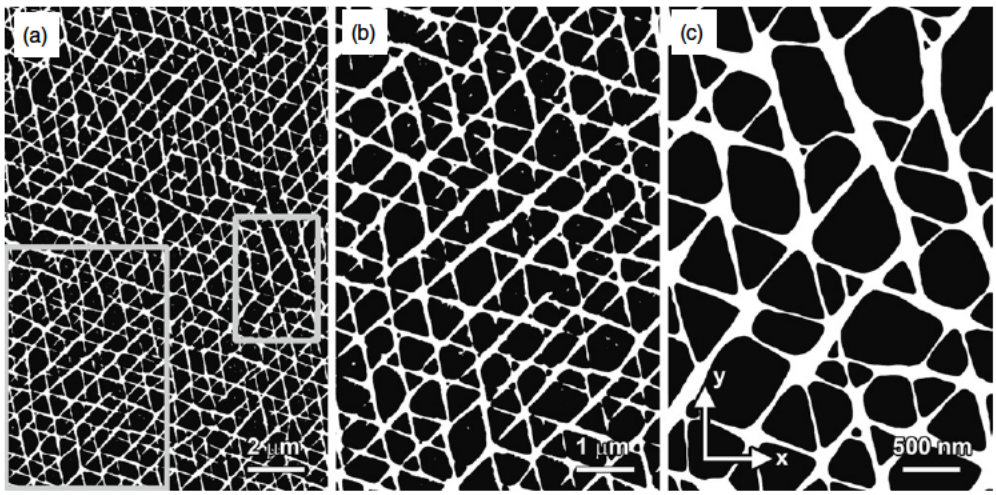

Figure 1. Binary images of γ' precipitate distributions obtained through segmentation of SEM images. The sample surface normal is $\{1\,1\,1\}$, and image dimensions are as follows: (*a*) 11×16.5, (*b*) 5.5×8.25 and (*c*) $2.75 \times 4.125\,\mu\text{m}^2$ in size. The x-axis is along $[3\,-4\,1]$ and the y-axis is along $[5\,2\,-7]$. The precipitates are in black and the matrix in white. The two gray insets in (*a*) indicate the 5.5×8.25 and $2.75 \times 4.125\,\mu\text{m}^2$ regions shown in (*b*) and (*c*).

hardening, occurs because of deviations from mean-field conditions for forest hardening in small volumes, thus biasing the statistics of ordinary dislocation processes [5, 10–12]. The key aspect of two-phase superalloy microcrystal behavior with respect to size effect is that the large scatter seen in fcc crystals is maintained while the strengthening effect is weaker [4]. Note that a weak size effect is unexpected, given the ubiquitous size effect reported in several fcc microcrystals. Rationalizing this behavior is the main objective of this work.

In this study, 2D dislocation dynamics simulations of the percolation of $a\langle 1\,1\,0\rangle$ superdislocation Frank–Read sources through an experimentally determined γ' precipitate distribution in micrometer-sized superalloys are used to examine the effect of sample size on the initial yield behavior (percolation threshold) as well as the scatter in the yield stress at each size [4]. Based on prior work where APB interaction was shown to be the dominant strengthening mechanism, only the APB interaction was considered for the precipitate–dislocation interaction, with an APB energy of $250\,\text{mJ}\,\text{m}^{-2}$ [13–15]. We carried out these simulations using the 3D massively parallel dislocation dynamics code ParaDiS [16], which was modified to account for the precipitate–dislocation APB interaction.

2. Method

Superdislocation Frank–Read sources, having random positions, sizes and orientations, were introduced on a $\{1\,1\,1\}$ glide plane of simulation cells having three different sizes, 2.75×4.125, 5.5×8.25 and $11 \times 16.5\,\mu\text{m}^2$. The superdislocation was divided into two $a/2\langle 1\,1\,0\rangle$ superpartials and each superpartial was divided into linear segments having a maximum size of $5a\langle 1\,1\,0\rangle$. The two superpartials were separated by 2 nm in the initial configuration. The Frank–Read source pinning points were constrained to lie in the matrix. Free surface boundary conditions were applied in the simulations [5]. The $\{1\,1\,1\}$ glide planes were populated with an experimentally determined size and spatial precipitate distribution, obtained from a scanning electron microscope (SEM) micrograph (see figure 1). The volume percent of γ' precipitates

in this superalloy was 73.5%. The precipitate distribution was voxelized into $2.75 \times 2.75\,\mathrm{nm}^2$ cells, with the cells digitized to a value of 0 or 1, corresponding to the matrix or precipitate phase, respectively.

The treatment of the APB interaction is as follows. If a dislocation node belonging to the leading superpartial lies inside a precipate voxel, a retarding force of γ per unit length is exerted on the node, where γ is the APB energy, since the leading superpartial forms an APB fault with its movement [13–15]. Likewise, if a dislocation node belonging to the trailing superpartial lies within a precipitate voxel, a positive force of γ per unit length is exerted on the dislocation node, where γ is the APB energy, since the trailing superpartial repairs an APB fault with its movement [13–15]. If the dislocation node is in the matrix, no precipitate force is exerted on the node. Constant stresses ranging from 600 to 1000 MPa in steps of 50 MPa, along a single-slip [1 2 3] direction, were applied on the dislocation. The minimum stress at which the Frank–Read source continuously moves through the {1 1 1} glide plane and multiplies was considered the percolation stress for the source. Thirty-six different random instantiations of the Frank–Read source were considered for the smallest size and twelve different instantiations were considered for the largest size. For the intermediate size, 2 different SEM micrographs were used to obtain the precipitate size and spatial positions and, for each micrograph, 12 different random instantiations of the Frank–Read source were simulated.

In all cases, at an APB energy of $250\,\mathrm{mJ\,m^{-2}}$, the mode of precipitate defeat in the simulations was bowing-assisted cutting rather than Orowan looping throughout the microstructure [13]. The precipitates were cut by the dislocations as superpartial pairs, with the trailing superpartial aiding the leading superpartial pair to enter the precipitate [13]. All the interactions between the leading and trailing superpartial pair segments were considered in the simulations [13]. For APB energies much higher than $250\,\mathrm{mJ\,m^{-2}}$ and/or for microstructures with much less volume fraction of precipitates than considered in the simulations, Orowan looping may occur [13]. The initial dislocation density in the superalloy sample, ρ, was $\sim 10^{11}$–$10^{12}\,\mathrm{m}^{-2}$ [4]. The contribution of forest dislocation interaction stress to initial yield, which can be estimated as $0.35\,\mu b\rho^{0.5}$ [17], where μ is the shear modulus and b is the Burgers vector of the superdislocation, is ~ 0.55–$1.75 \times 10^{-4}\mu$ and is neglected in the analysis. The strength of micrometer-sized crystals of superalloys, σ_{S}, within the single-arm source model can be written as [5]

$$\sigma_{\mathrm{S}} = \sigma_{\mathrm{ssp}} + \sigma_{\mathrm{f}} + \sigma_{\mathrm{ex}} \tag{1}$$

where σ_{ssp} is the single-arm source percolation stress in the presence of precipitates, σ_{f} is the friction stress from solid-solution hardening in the matrix and σ_{ex} is the exhaustion hardening from dislocation–dislocation interactions and exhaustion of initially operating single-arm dislocation sources. To achieve a plastic strain of 0.2%, a single-arm source needs to traverse through a 2.5 μm crystal approximately 30 revolutions, 5.0 μm crystal 60 revolutions and a 10.0 μm crystal 120 revolutions. For such small plastic strains, we assume that dislocation interactions are negligible and ignore the exhaustion hardening contribution. We use 2D dislocation dynamics to determine the single-arm source percolation stress in the presence of precipitates, σ_{ssp}, for three different sample sizes described before, and add a friction stress of 250 MPa [18] to estimate the experimental 0.2% flow stress at each size. Prior work has shown that matrix stress influences the percolation stress in a linear fashion, as assumed here [13].

3. Results and discussion

Figure 2 is a plot of the critical percolation stress as a function of size obtained for the Frank–Read sources for the present 2D dislocation dynamics simulations using a matrix friction

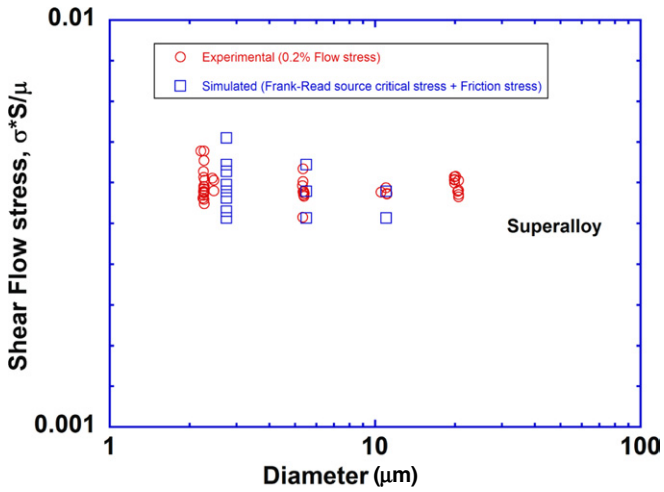

Figure 2. Critical percolation stress as a function of size obtained for the Frank–Read sources with the present 2D dislocation dynamics simulations plus matrix friction stress of ∼250 MPa, as well as the experimental 0.2% yield stress data for the same superalloy, multiplied by the Schmid factor and scaled by the shear modulus.

stress [18] of ∼250 MPa [10]. The plot includes the experimental 0.2% yield stress data for the same superalloy, multiplied by the Schmid factor and scaled by the shear modulus, ∼79 GPa [4]. Two trends can be observed on this plot: one, a weakly increasing yield stress with decreasing size, and two, the relative scatter in yield stress at each size is similar between the simulations and experiments. For most of the simulation results, the Frank–Read source bows, interacts with the surface and forms two single-arm sources. Subsequently, the weaker of the two single-arm sources, with one end pinned inside the crystal and the other end on the surface, controls the critical percolation stress for the superdislocation. In some cases, the initial Frank–Read source is the critical configuration, where both ends are pinned inside the crystal.

Figure 3 shows a plot of the critical stress obtained for the 36 different instantiations of the Frank–Read source at $2.75 \times 4.125\ \mu\text{m}^2$ size, versus b/l, where l is the single-arm source length at the critical configuration. If the critical configuration is a Frank–Read source, its effective single-arm source length is taken to be half the length of the Frank–Read source [19]. A linear fit to the critical stress data gives an equation of the form

$$\sigma \sim 668\,\text{MPa} + (0.68/S)\mu b/l \tag{2}$$

where S is the Schmid factor. In equation (2), 668 MPa is the critical stress at an infinite single-arm source length and can be taken to be the precipitation hardening contribution for an infinite material. This value, in combination with a solid-solution hardening component of ∼250 MPa, corresponds closely to the minimum in critical stress observed for larger sizes (see figure 2). The second term, $(0.68/S)\mu b/l$, is interpreted as the hardening contribution from the single-arm source and corresponds closely to the calculated results for single-arm sources given in [19]. However, figure 3 shows that there is a significant amount of scatter, about the average straight line fit given by equation (2), which is a result of precipitate size and spatial distribution.

Figure 4 shows the critical single-arm source configurations for two different instantiations of the Frank–Read source in the $2.75 \times 4.125\ \mu\text{m}^2$ cell, along with the precipitate configuration.

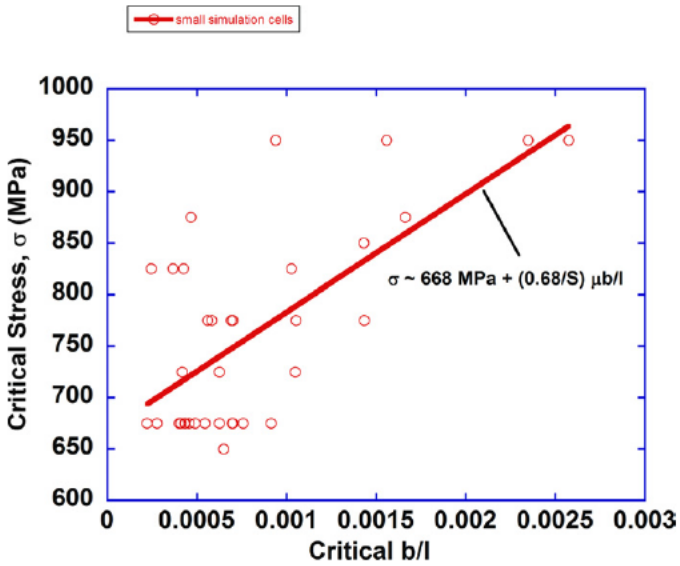

Figure 3. Critical stress, σ obtained for 36 different instantiations of the Frank–Read source with a size of $2.75 \times 4.125\ \mu m^2$, versus b/l, where l is the effective single-arm source length at the critical configuration.

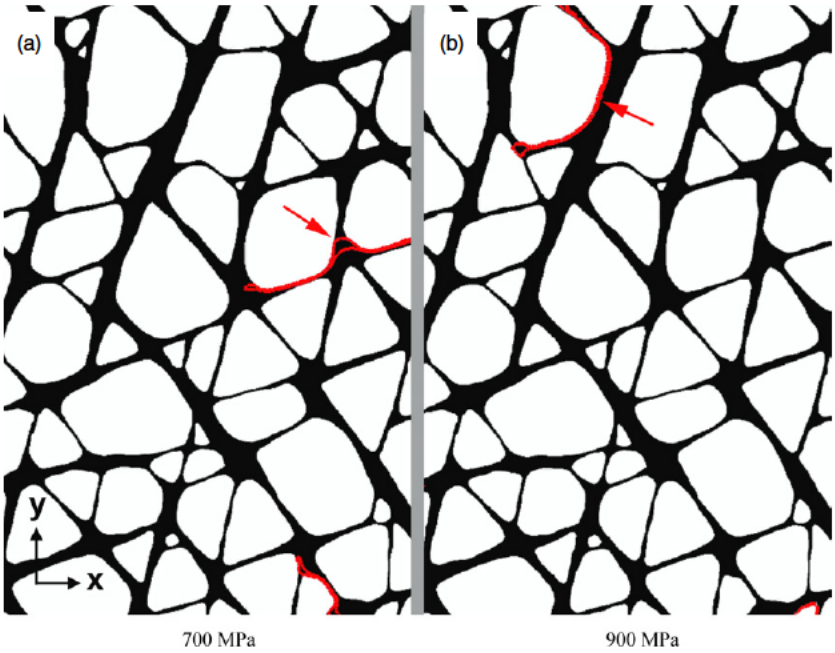

Figure 4. Images of the critical single-arm source configurations for two different instantiations of the Frank–Read source in the $2.75 \times 4.125\ \mu m^2$ cell, along with the precipitate configuration. The x-axis is along [3 −4 1] and the y-axis is along [5 2 −7]. The precipitates are in white and the matrix in black. The arrows point to the critical single-arm source configurations.

For the two cases, the critical single-arm source lengths are almost identical and equal to ∼1100 nm. However, the critical stress in one case is 900 MPa, whereas in the second case it is much lower and equal to 700 MPa. Examination of the precipitate configuration at the critical single-arm source positions for the two examples shows that they are significantly different. For the instantiation having the higher critical stress, the single-arm source is almost completely blocked by the precipitate. In the second case, where the critical stress is lower, the single-arm source is only partially blocked by the precipitates. This result suggests that the specific precipitate structure at the critical single-arm source positions is an important factor in determining the critical stress. This effect in superalloys can cause the precipitation hardening contribution to increase from the infinite material value, $1/S(\gamma/2b)f$, where f is a fraction less than 1, to a situation where the superdislocation single-arm source is completely blocked by precipitates, $1/S(\gamma/2b)$. Critical single-arm source configurations and sizes for which the statistics of the channels in the precipitate distribution are significantly different from those for an infinite material are expected to show this effect. Therefore, the size effect and scatter in yield stress of superalloys are related to two factors: the strength of the single-arm sources and the variation in precipitate structure at the single-arm source positions. The stress, $1/S(\gamma/2b)$, plus any solid-solution strengthening in the precipitate can be taken to be the limiting stress value, beyond which there will not be any strengthening in micrometer-sized crystals of superalloys. Such a condition is valid for the assumptions that the stress to nucleate superdislocations at a surface is low and the mobility of freshly nucleated superdislocations controls the yield stress [20]. However, the experimental data [4] do not show any such tendency for a saturation stress value, most likely because the experimental size-effect data do not include small enough sizes of micrometer-sized crystals of superalloys.

It is appropriate to point out the assumptions used in this work. First, we note that the APB energy of the experimental superalloy is unknown. The measured and calculated APB energy of various superalloys typically range from 180 to 320 mJ m^{-2} [18]. Second, the solid-solution-hardening contribution assumed in the comparison of simulation with the experimental data is calculated from matrix chemistry and known dependences. Third, the strain-hardening effects from forest dislocations as well as thermally activated processes like cross-slip in the γ matrix or γ' precipitate were not considered in the simulations. In light of these considerations, it is suggested that the modified source-truncation mechanism be taken as one possible explanation for the observed weak size effect in initial yield, as well as the scatter in yield stress at each size in experiments of micrometer-sized crystals of superalloys. From simulation results shown in figure 4, one can infer that the scatter arises from the statistics of precipitate distribution along the truncated dislocation segment at the location of criticality.

Acknowledgments

The authors acknowledge the use of the 3D dislocation dynamics code, ParaDiS, which was developed at the Lawrence Livermore National Laboratory by Dr Vasily Bulatov and co-workers. This work was supported by AFOSR, and by a grant of computer time from the DOD High Performance Computing Modernization Program, at the Aeronautical Systems Center/Major Shared Resource Center.

References

[1] Uchic M D, Dimiduk D M, Florando J and Nix W D 2004 *Science* **305** 986
[2] Greer J R, Oliver W C and Nix W D 2005 *Acta Mater.* **53** 1821
[3] Volkert C A and Lilliodden E 2006 *Phil. Mag.* **86** 5567

[4] Shade P A, Uchic M D, Dimiduk D M, Viswanathan G B, Wheeler R and Fraser H L 2011 *Mater. Sci. Eng.* A **535** 53
[5] Rao S I, Dimiduk D M, Parthasarathy T A, Uchic M D, Tang M and Woodward C 2008 *Acta Mater.* **56** 3245
[6] Senger J, Weygand D, Gumbsch P and Kraft O 2008 *Scr. Mater.* **58** 587
[7] Tang H, Schwarz K W and Espinosa H D 2007 *Acta Mater.* **55** 1607
[8] Zhou C, Biner S and Lesar R 2010 *Acta Mater.* **58** 1565
[9] Nadgorny E M, Dimiduk D M and Uchic M D 2008 *J. Mater. Res.* **23** 2829
[10] Dimiduk D M, Uchic M D and Parthasarathy T A 2005 *Acta Mater.* **53** 4065
[11] Sevillano J G, Arizcorreta I O and Kubin L P 2001 *Mater. Sci. Eng.* A **309–310** 393
[12] Norfleet D M, Dimiduk D M, Polasik S J, Uchic M D and Mills M J 2008 *Acta Mater.* **56** 2988
[13] Rao S I, Parthasarathy T A, Dimiduk D M and Hazzledine P M 2004 *Phil. Mag.* **84** 3195
[14] Vattre A, Devincre B and Roos A 2009 *Intermetallics* **17** 988
[15] Vattre A, Devincre B and Roos A 2010 *Acta Mater.* **58** 1938
[16] Arsenlis A, Cai W, Tang M, Rhee M, Oppelstrup T, Hommes G, Pierce T G and Bulatov V V 2007 *Modelling Simul. Mater. Sci. Eng.* **15** 553
[17] Madec R, Devincre B and Kubin L P 2002 *Phys. Rev. Lett.* **89** 255508
[18] Parthasarathy T A, Rao S I and Dimiduk D M 2004 *Superalloys 2004* ed K A Green *et al* (Warrendale, PA: The Minerals, Metals and Materials Society) p 887
[19] Rao S I, Dimiduk D M, Tang M, Parthasarathy T A, Uchic M D and Woodward C 2007 *Phil. Mag.* **87** 4777
[20] Parthasarathy T A, Rao S I, Dimiduk D M, Uchic M D and Trinkle D R 2007 *Scr. Mater.* **56** 313